SYSTEM RESPONSE KERNEL CALCULATION FOR LIST-MODE RECONSTRUCTION IN STRIP PET DETECTOR*

P. Białas[a], J. Kowal[a], A. Strzelecki[a], T. Bednarski[a]
E. Czerwiński[a], Ł. Kapłon[a], A. Kochanowski[a], G. Korcyl[a]
P. Kowalski[b], T. Kozik[a], W. Krzemień[a], M. Molenda[a]
P. Moskal[a], Sz. Niedźwiecki[a], M. Pałka[a], M. Pawlik[a]
L. Raczyński[b], Z. Rudy[a], P. Salabura[a], N.G. Sharma[a]
M. Silarski[a], A. Słomski[a], J. Smyrski[a], W. Wiślicki[b]
M. Zieliński[a]

[a]The Marian Smoluchowski Institute of Physics, Jagiellonian University
Reymonta 4, 30-059 Kraków, Poland
[b]Świerk Computing Centre, National Centre for Nuclear Research
05-400 Otwock-Świerk, Poland

(Received September 5, 2013)

Reconstruction of the image in Positron Emission Tomographs (PET) requires the knowledge of the system response kernel which describes the contribution of each pixel (voxel) to each tube of response (TOR). This is especially important in list-mode reconstruction systems, where an efficient analytical approximation of such function is required. In this contribution, we present a derivation of the system response kernel for a novel 2D strip PET.

DOI:10.5506/APhysPolBSupp.6.1027
PACS numbers: 87.85.Pq, 87.57.Q–, 87.57.C–, 87.57.N–

1. Introduction

The Positron Emission Tomograph (PET) works by estimating the radioactive fluid density (tracer) from the measurements of the γ quanta emitted from the beta plus (β^+) decay. The two quanta are emitted simultaneously and almost back-to-back. We will call such emission an *event*. The γ are detected in the detectors surrounding the patient. Detecting two quanta yields a *tube of response* passing through the emission point. The better the

* Presented at the Symposium on Applied Nuclear Physics and Innovative Technologies, Kraków, Poland, June 3–6, 2013.

spatial resolution of the detection the thinner is the tube giving a better reconstruction. Currently, all PET scanners perform the measurements using the non-organic scintillating crystals and the spatial resolution is controlled by the crystal size which can be as small as few millimeters across.

Our group is working currently on a prototype PET using the long plastic scintillator strips where the spatial resolution is obtained from the time-of-flight measurements [3–5]. Achieving sufficient time resolution (less than 100 ps) is the main technological challenge, however, the novel hardware requires also the suitable adaptation of the reconstruction algorithm.

This contribution is concerned with the calculation of the system kernel in the 2D image reconstruction in the axial plane of our strip PET detector. It is organized as follows: in Section 2 we describe the detector geometry and measurement errors, in Section 3 the principles of the List-mode Expectation Maximization Algorithm is described, and in the following sections we derive the system response kernel.

2. Detector geometry

In its final form, our detector should consist of strips of scintillators arranged on a cylinder. The strips are aligned with the axis of the cylinder. We will start with a simpler 2D geometry — two parallel line segments of scintillators of the length L at the distance $2\bar{R}$ (see figure 1). This is, anyway, a necessary step as our first prototype will consist of two bars of scintillators. This is, in a sense, a minimal configuration required for testing. The real idealization here is neglecting the scintillator thickness.

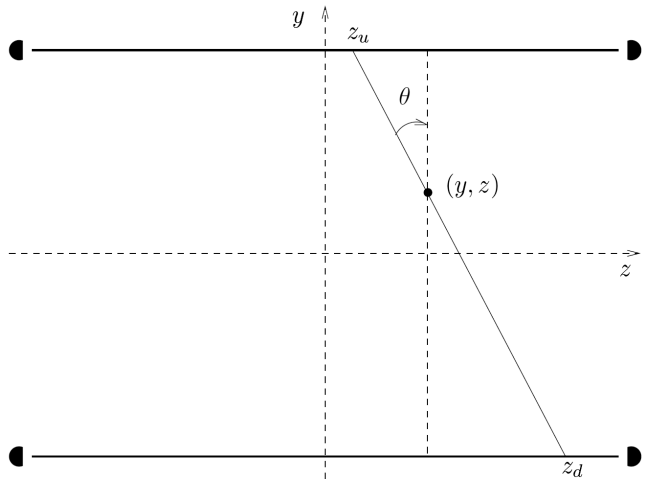

Fig. 1. Detector geometry.

A photomultiplier tube is attached to the end of each strip. The γ quanta can scatter in the scintillator and produce light which then propagates along the scintillator to the photomultipliers. By measuring the time at which light reaches the photomultiplier, we can estimate the position at which γ had crossed the scintillator

$$\widetilde{z_u} = \tfrac{1}{2}\, c_{\mathrm{sci}} \left(\widetilde{T}_{ul} - \widetilde{T}_{ur} \right) , \qquad \widetilde{z_d} = \tfrac{1}{2}\, c_{\mathrm{sci}} \left(\widetilde{T}_{dl} - \widetilde{T}_{dr} \right) . \tag{1}$$

We use tildas to mark the measured quantities as opposed to the exact ones. The c_{sci} denotes the effective speed of light in the scintillator. It takes into account both the actual speed of light in scintillator and the elongation of the optical path due to reflections. We have estimated this to be approximately 1.3×10^8 m/s for the scintillators we use. Combining the time measurements from the two scintillators, we can estimate the position of the emission point on the line joining the upper and lower crossing points

$$\widetilde{\Delta l} = \tfrac{1}{2}\, c \left(\left(\widetilde{T}_{ul} + \widetilde{T}_{ur} \right) - \left(\widetilde{T}_{dl} + \widetilde{T}_{dr} \right) \right) , \tag{2}$$

where Δl is the difference of distances of the reconstructed point (y, z) from the upper and lower detection points (see figure 1).

Those quantities are, of course, subject to measurement errors and are related to exact ones by

$$\widetilde{z}_y = z_y + \varepsilon_{z_y} , \qquad y = u, d , \qquad \widetilde{\Delta l} = \Delta l + \varepsilon_{\Delta l} . \tag{3}$$

We assume that the errors ε are normally distributed with some correlation matrix C. In general, the magnitude of the errors will depend on the place, where the γ hit the scintillator $C = C(z_u, z_d)$. This matrix is a necessary and important input for the reconstruction algorithm. Under some plausible assumptions, which are beyond the scope of this contribution, this matrix can be parametrized by three functions

$$C = \begin{pmatrix} \sigma_z^2(z_u) & 0 & \gamma(z_u) \\ 0 & \sigma_z^2(z_d) & -\gamma(z_d) \\ \gamma(z_u) & -\gamma(z_d) & \sigma_{\Delta l}^2(z_u, z_d) \end{pmatrix} , \tag{4}$$

where

$$\sigma_z^2(z) = \left\langle \varepsilon_{u(d)}^2(z) \right\rangle , \qquad \sigma_{\Delta l}^2(z_u, z_d) = \left\langle \varepsilon_{\Delta l}^2(z_u, z_d) \right\rangle \tag{5}$$

and

$$\gamma(z) = \left\langle \varepsilon_{z_u}(z) \varepsilon_{\Delta l}(z, z_d) \right\rangle = - \left\langle \varepsilon_{z_d}(z) \varepsilon_{\Delta l}(z_u, z) \right\rangle . \tag{6}$$

The z_u, z_d and Δl are related to the coordinates (y, z) of the emission point and the emission angle θ by the formulas

$$\begin{aligned} z_u &= z + \left(\bar{R} - y\right) \tan\theta \,, \\ z_d &= z - \left(\bar{R} + y\right) \tan\theta \,, \\ \Delta l &= -2y\sqrt{1 + \tan^2\theta} \,, \end{aligned} \tag{7}$$

and, conversely,

$$\begin{aligned} \tan\theta &= \frac{z_u - z_d}{2\bar{R}} \,, \\ y &= -\frac{1}{2}\frac{\Delta l}{\sqrt{1 + \tan^2\theta}} = \frac{2\bar{R}\Delta l}{\sqrt{z_u - z_d + 4\bar{R}^2}} \,, \\ z &= \frac{1}{2}\left(z_u + z_d + 2y\tan\theta\right) = \frac{1}{2}\left(z_u + z_d + \frac{(z_u - z_d)\Delta l}{\sqrt{z_u - z_d + 4\bar{R}^2}}\right) . \end{aligned} \tag{8}$$

3. List-mode reconstruction

Given good enough time resolution, our detector using the time-of-flight technique could reconstruct each individual event with sufficient accuracy to measure the emitter density directly. Currently, however, this is not the case and the measurements errors have to be incorporated into the reconstruction using a *statistical* approach. Almost every current reconstruction algorithm is based on likelihood maximization approach described in [6, 7]. This work is concerned with *binned* data. However, because of the advance of the technology most of the scanners work in the list-mode where every single detected event is recorded separately. The extensions of the likelihood maximization approach to this case was done in [1, 2].

Here, we provide a very brief introduction to this algorithm, for details the Reader is referred to [2]. Let us denote the *system response kernel* by $P(\widetilde{\boldsymbol{e}}|i)$. This is defined as probability that a *detected* event emitted from pixel i was reconstructed as $\widetilde{\boldsymbol{e}}$. Given this probability for each emitter density ρ, we can calculate the probability of observing the particular set of N events [1]

$$P\left(\{\widetilde{\boldsymbol{e}}_1, \ldots, \widetilde{\boldsymbol{e}}_N\}\,|\rho\right) = \prod_j \sum_i P\left(\widetilde{\boldsymbol{e}}_j|i\right) \frac{\rho(i)s(i)}{\sum_i \rho(i)s(i)} \,. \tag{9}$$

The $s(i)$ is the *sensitivity* of the pixel *e.g.* the probability that an event originating from pixel i will be detected at all. Together $s(i)$ and $P(\widetilde{\boldsymbol{e}}_j|i)$ provide the complete model of the detector.

The reconstruction algorithm consists of finding the distribution ρ that maximizes this probability, or more accurately its logarithm — the likelihood. That is achieved using the iterative Expectation Maximization (EM) algorithm [2]

$$\rho(l)^{(t+1)} = \sum_{j=1}^{N} \frac{P(\widetilde{\boldsymbol{e}}_j|l)\rho(l)^t}{\sum\limits_{i=1}^{M} P(\widetilde{\boldsymbol{e}}_j|i)s(i)\rho(i)^t} \,. \tag{10}$$

The sum over j runs over all collected events $\{\widetilde{\boldsymbol{e}}_j\}$. Considering that up to hundred millions of events can be collected during a single scan, this is a very time-consuming calculation. Finding an efficient approximation for the system response kernel is of a paramount importance.

4. System response kernel

To calculate $P(\widetilde{\boldsymbol{e}}|i)$, we start with $p(\widetilde{\boldsymbol{e}}|\boldsymbol{e})$ — the probability that an event $\boldsymbol{e}$ will be detected as $\widetilde{\boldsymbol{e}}$. This includes the possibility of an event not being detected

$$s(\boldsymbol{e}) \equiv \int d\,\widetilde{\boldsymbol{e}}\, p(\widetilde{\boldsymbol{e}}|\boldsymbol{e}) \leq 1 \,. \tag{11}$$

The $s(\boldsymbol{e})$ is the sensitivity of an event — the probability that the event will be detected. With this definition

$$P(\widetilde{\boldsymbol{e}}|i) = \frac{p(\widetilde{\boldsymbol{e}}|i)}{s(i)} \,, \tag{12}$$

where

$$p(\widetilde{\boldsymbol{e}}|i) = \pi^{-1} \int\limits_{y,z\in i} \int d\,\theta\, p(\widetilde{\boldsymbol{e}}|y,z,\theta) \tag{13}$$

and

$$s(i) = \pi^{-1} \int d\,\widetilde{\boldsymbol{e}}\, p(\widetilde{\boldsymbol{e}}|i) = \int\limits_{y,z\in i} \int d\,\theta\, s(y,z,\theta) \,. \tag{14}$$

We assume that every event reaching the detector is detected so the $s(\boldsymbol{e})$ is given solely by the geometrical constraints

$$s(\boldsymbol{e}) = \begin{cases} 1 & z_u \in [-L/2, L/2] \wedge z_d \in [-L/2, L/2] \\ 0 & \text{otherwise} \end{cases} \,. \tag{15}$$

This is somewhat more complicated in the image space

$$s(y,z,\theta) = \begin{cases} 1 & \tan\theta \in \left[\max\left(-\frac{\frac{1}{2}L+z}{R-y}, \frac{-\frac{1}{2}L+z}{R+y}\right) \,, \quad \min\left(\frac{\frac{1}{2}L-z}{R-y}, \frac{\frac{1}{2}L+z}{R+y}\right)\right] \\ 0 & \text{otherwise} \end{cases} \,. \tag{16}$$

We will also need the sensitivity of the image point (y,z)

$$s(y,z) = \pi^{-1} \int d\,\theta\, s(y,z,\theta) = \pi^{-1}(\theta_{\max} - \theta_{\min}) \tag{17}$$

with

$$\begin{aligned} \theta_{\min} &= \arctan\max\left(-\frac{\frac{1}{2}L+z}{R-y}, \frac{-\frac{1}{2}L+z}{R+y}\right), \\ \theta_{\max} &= \arctan\min\left(\frac{\frac{1}{2}L-z}{R-y}, \frac{\frac{1}{2}L+z}{R+y}\right). \end{aligned} \tag{18}$$

As discussed in the previous section, the errors are normally distributed

$$p(\widetilde{\boldsymbol{e}}|\boldsymbol{e}) = s(\boldsymbol{e}) \frac{\det^{-\frac{1}{2}} C(\boldsymbol{e})}{(2\pi)^{\frac{3}{2}}} \exp\left(-\frac{1}{2}(\widetilde{\boldsymbol{e}}-\boldsymbol{e})^T C^{-1}(\boldsymbol{e})(\widetilde{\boldsymbol{e}}-\boldsymbol{e})\right), \tag{19}$$

where

$$\Delta\boldsymbol{e} = \boldsymbol{e}(z,y,\theta) - \boldsymbol{e}\left(\widetilde{z},\widetilde{y},\widetilde{\theta}\right) = \begin{pmatrix} z + \left(\bar{R}-y\right)\tan\theta - \widetilde{z} - \left(\bar{R}-\widetilde{y}\right)\tan\widetilde{\theta} \\ z - \left(\bar{R}+y\right)\tan\theta - \widetilde{z} + \left(\bar{R}+\widetilde{y}\right)\tan\widetilde{\theta} \\ -2y\sqrt{1+\tan^2\theta} + 2\widetilde{y}\sqrt{1+\tan^2\theta} \end{pmatrix}. \tag{20}$$

We will now construct an approximation for the formula (12). We start by calculating

$$p(\widetilde{\boldsymbol{e}}|y,z) = \pi^{-1} \int d\,\theta\, p(\widetilde{\boldsymbol{e}}|y,z,\theta)\,. \tag{21}$$

The first approximation we make is to assume that the correlation matrix C is depending weakly on $\boldsymbol{e}$ and we can approximate it by its value at $\widetilde{\boldsymbol{e}}$. The integral (21) becomes then

$$p(\widetilde{\boldsymbol{e}}|y,z) = \pi^{-1} \frac{\det^{-\frac{1}{2}} C(\widetilde{\boldsymbol{e}})}{(2\pi)^{\frac{3}{2}}} \int d\,\theta\, s(\boldsymbol{e}) \exp\left(-\frac{1}{2}(\widetilde{\boldsymbol{e}}-\boldsymbol{e})^T C^{-1}(\widetilde{\boldsymbol{e}})(\widetilde{\boldsymbol{e}}-\boldsymbol{e})\right). \tag{22}$$

We will approximate this integral using the saddle-point approximation. To this end, we first expand the $\Delta\boldsymbol{e}$ in

$$\Delta\theta = \theta - \widetilde{\theta}\,, \tag{23}$$

$$\Delta\boldsymbol{e} \approx \vec{o}\Delta\theta^2 + \vec{a}\Delta\theta + \vec{b} \tag{24}$$

with

$$\vec{o} = \begin{pmatrix} -(\Delta y + \widetilde{y} - R)\tan\widetilde{\theta}\cos^{-2}\widetilde{\theta} \\ -(\Delta y + \widetilde{y} + R)\tan\widetilde{\theta}\cos^{-2}\widetilde{\theta} \\ -(\Delta y + \widetilde{y})\cos^{-1}\widetilde{\theta}\left(1 + 2\tan^2\widetilde{\theta}\right) \end{pmatrix}, \tag{25}$$

$$\vec{a} = \begin{pmatrix} -(\Delta y + \widetilde{y} - R)\cos^{-2}\widetilde{\theta} \\ -(\Delta y + \widetilde{y} + R)\cos^{-2}\widetilde{\theta} \\ -2(\Delta y + \widetilde{y})\cos^{-1}\widetilde{\theta}\tan\widetilde{\theta} \end{pmatrix}, \tag{26}$$

and

$$\vec{b} = \begin{pmatrix} \Delta z - \Delta y\tan\widetilde{\theta} \\ \Delta z - \Delta y\tan\widetilde{\theta} \\ -2\Delta y\cos^{-1}\widetilde{\theta} \end{pmatrix}, \tag{27}$$

where

$$\Delta y = y - \widetilde{y} \qquad \text{and} \qquad \Delta z = z - \widetilde{z}\,. \tag{28}$$

After inserting (24) into the exponent of (22), we obtain the expression

$$\tfrac{1}{2}\left(\vec{o}\Delta\theta^2 + \vec{a}\Delta\theta + \vec{b}\right) C^{-1}\left(\vec{o}\Delta\theta^2 + \vec{a}\Delta t + \vec{b}\right) \tag{29}$$

which we truncate to the quadratic order

$$\left(\vec{o}\,C^{-1}\vec{b} + \tfrac{1}{2}\vec{a}\,C^{-1}\vec{a}\right)\Delta\theta^2 + \vec{a}\,C^{-1}\vec{b}\,\Delta\theta + \tfrac{1}{2}\vec{b}\,C^{-1}\vec{b}\,. \tag{30}$$

After differentiating with respect to $\Delta\theta$, we obtain the equation for the minimum

$$\left(2\vec{o}\,C^{-1}\vec{b} + \vec{a}\,C^{-1}\vec{a}\right)\Delta\theta + \vec{a}\,C^{-1}\vec{b} = 0 \tag{31}$$

with the solution

$$\Delta\theta_{\min} = -\frac{\vec{b}\,C^{-1}\vec{a}}{\vec{a}\,C^{-1}\vec{a} + 2\vec{o}\,C^{-1}\vec{b}}\,. \tag{32}$$

Denoting

$$\tau = \Delta\theta - \Delta\theta_{\min}\,, \tag{33}$$

we rewrite Eq. (30) as

$$\frac{1}{2}\left(\vec{a}\,C^{-1}\vec{a} + 2\vec{o}\,C^{-1}\vec{b}\right)\tau^2 + \frac{1}{2}\left(\vec{b}\,C^{-1}\vec{b} - \frac{\left(\vec{a}\,C^{-1}\vec{b}\right)^2}{\vec{a}\,C^{-1}\vec{a} + 2\vec{o}\,C^{-1}\vec{b}}\right). \tag{34}$$

Finally, we obtain

$$p(\widetilde{\boldsymbol{e}}|y,z) \;\approx\; \frac{\det{}^{-\frac{1}{2}} C(\widetilde{\boldsymbol{e}})}{(2\pi)^{\frac{3}{2}}} \exp\left(-\frac{1}{2}\left(\vec{b}\,C^{-1}\vec{b} - \frac{\left(\vec{b}\,C^{-1}\vec{a}\right)^2}{\vec{a}\,C^{-1}\vec{a} + 2\vec{o}\,C^{-1}\vec{b}}\right)\right)$$
$$\times\pi^{-1}\int d\tau\, s(y,z,\theta)\, \exp\left(-\frac{1}{2}\tau^2\left(\vec{a}\,C^{-1}\vec{a} + 2\vec{o}\,C^{-1}\vec{b}\right)\right). \quad (35)$$

If we assume that $\widetilde{\boldsymbol{e}}$ is sufficiently far from the edge of the detector, then we can neglect the sensitivity factor $s(y,z,\theta)$, and after Gaussian integration we obtain

$$p(\widetilde{\boldsymbol{e}}|y,z) \;\approx\; \frac{\det{}^{-\frac{1}{2}} C}{2\pi\sqrt{\vec{a}\,C^{-1}\vec{a} + 2\vec{o}\,C^{-1}\vec{b}}}\pi^{-1}$$
$$\times\exp\left(-\frac{1}{2}\left(\vec{b}\,C^{-1}\vec{b} - \frac{\left(\vec{b}\,C^{-1}\vec{a}\right)^2}{\vec{a}\,C^{-1}\vec{a} + 2\vec{o}\,C^{-1}\vec{b}}\right)\right). \quad (36)$$

We still need to perform the integration over the pixel. We will just approximated it by the value of (36) at its center

$$p(\widetilde{\boldsymbol{e}}|i) \approx V(i)p(\widetilde{\boldsymbol{e}}|y_i,z_i) \quad (37)$$

and

$$P(\widetilde{\boldsymbol{e}}|i) \approx \frac{p(\widetilde{\boldsymbol{e}}|y_i,z_i)}{s(y_i,z_i)}, \quad (38)$$

where (y_i,z_i) denotes the center of pixel i.

5. Validation

To validate our calculations, we compare the formulas (13) and (36) for few selected events. The biggest issue here is the estimation of the correlation matrix C. We will consider the case of diagonal correlation matrix not depending on the positions

$$C^{-1} = \begin{pmatrix} \frac{1}{\sigma_z^2} & 0 & 0 \\ 0 & \frac{1}{\sigma_z^2} & 0 \\ 0 & 0 & \frac{1}{\sigma_{\Delta l}^2} \end{pmatrix}. \quad (39)$$

From our measurements, we estimate

$$\sigma_z \approx 10\ \text{mm}, \qquad \sigma_{\Delta l} \approx 63\ \text{mm}. \quad (40)$$

We then consider events with $y = 300$ mm and angles zero, and 45° (see figure 2). The $z = 0$ and 300 respectively. For the detector, we use $R = 450\,\text{mm}$ and $L = 1000\,\text{mm}$.

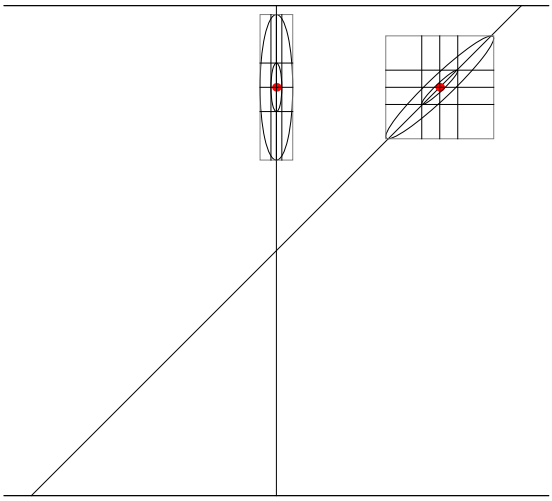

Fig. 2. Two of the events used for validation. The reconstructed point is at $\widetilde{y} = 300$ mm and reconstructed angles are 0° and 45°.

It is clear that the formula (36) is non-negligible only in a limited region around the reconstruction point. To estimate this region, we will use only the first term from the exponent. This a homogeneous polynomial of the second order in Δy and Δz so it defines a ellipse around reconstruction point given by the equation

$$\vec{b}\, C^{-1} \vec{b} = R^2\,. \tag{41}$$

The region of the interest is defined as the three sigma ellipse ($R = 3$).

For each event, we scan the formulas (13) and (36) along the horizontal and vertical line segments based on the bounding box of the one σ ellipse (see figure 2). For this choice of parameters, the two formulas were practically indistinguishable.

6. Summary

We have presented a derivation of the system response kernel for a PET detector based on time-of-flight measurements in two parallel scintillators strips. The resulting formula for the kernel is still quite complicated. For each event, the expression in the exponent is a rational function in variables Δy and Δz. We could envisage further simplification, but this can

be problematic without detailed knowledge of the detector geometry/size and the matrix $C(\boldsymbol{e})$. However, we believe that our formula provides a very good starting point for further approximations once the detector geometry is fixed.

The biggest simplification we have made is to assume that the scintillators have no thickness. In reality, they can be up to 20 mm thick. A simplest approach would be to incorporate this into the correlation matrix. However, our preliminary calculations show that the resulting errors are not Gaussian. This is a subject of an ongoing investigation.

We acknowledge technical and administrative support by M. Adamczyk, T. Gucwa-Ryś, A. Heczko, K. Łojek, M. Kajetanowicz, G. Konopka-Cupiał, J. Majewski, W. Migdał, and the financial support by the Polish National Center for Development and Research and by the Foundation for Polish Science through MPD programme, the EU and MSHE Grant No. POIG.02.03.00-00-013/09.

REFERENCES

[1] H.H. Berret, T. White, L. Parra, *J. Opt. Soc. Am.* **A14**, 2914 (1997).

[2] L. Parra, H.H. Berret, *IEEE Trans. Med. Imaging* **17**, 228 (1998).

[3] P. Moskal *et al.*, *Bio-Algorithms and Med-Systems* **7**, 73 (2011) [arXiv:1305.5187 [physics.med-ph]].

[4] P. Moskal *et al.*, *Nucl. Med. Rev.* **C15**, 68 (2012) [arXiv:1305.5562 [physics.ins-det]].

[5] P. Moskal *et al.*, *Nucl. Med. Rev.* **C15**, 81 (2012) [arXiv:1305.5559 [physics.ins-det]].

[6] L.A. Shepp, Y. Vardi, *IEEE Trans. Med. Imaging* **1**, 113 (1982).

[7] L.A. Shepp, Y. Vardi, L. Kaufman, *J. Am. Stat. Assoc.* **80**, 8 (1985).